npj | precision oncology

Article

Published in partnership with The Hormel Institute, University of Minnesota

https://doi.org/10.1038/s41698-025-00904-x

FOXA1-dependent NSUN2 facilitates the advancement of prostate cancer by preserving TRIM28 mRNA stability in a m5C-dependent manner

Zhenda Wang[1,2,6], Abudurexiti Mierxiati[3,6], Wenkai Zhu[4], Tian Li[5] ✉, Hua Xu[1,2] ✉, Fangning Wan[1,2] ✉ & Dingwei Ye[1,2] ✉

RNA epigenetics is gaining increased attention for its role in the initiation, metastasis, and drug resistance of tumors. These studies have primarily focused on m6A modification. However, despite being the second most abundant modification found in RNA, the role of m5C modification in prostate cancer remains largely unexplored. Here, we predict an RNA m5C methyltransferase, NSUN2, as a potential therapeutic target for prostate cancer using various bioinformatics approaches, and verify the potential of NSUN2 as a target through multiple preclinical models. Mechanistically, NSUN2 enhances the stability of TRIM28 mRNA by adding m5C modification, promoting the expression of TRIM28. Concurrently, FOXA1, a prostate cancer lineage-specific transcription factor, transcriptionally activates the expression of NSUN2. Our study confirms the clinical potential of targeting RNA epigenetics for the treatment of prostate cancer and elucidates, mechanistically, how RNA epigenetics participates in the complex biological activities within tumors via the FOXA1-NSUN2-TRIM28 axis.

The most prevalent histological form of prostate cancer[1,2] is called prostate adenocarcinoma (PRAD), and it can be identified by its persistent reliance on the androgen receptor (AR) signaling pathway[3] Androgen deprivation therapy (ADT) has therefore become the main therapeutic option[4]. Despite improvements in survival rates, almost every patient eventually results in castration-resistant prostate cancer (CRPC), which is marked by the rapid establishment of resistance to ADT[5–7]. Recent years have witnessed advancements in treatment choices, including abiraterone, enzalutamide, apalutamide, and darolutamide[8–13]. Nevertheless, they are not consistently therapeutic. This treatment resistance is ascribed to a complex interplay of mechanisms, including reactivation of the androgen receptor pathway, activation of alternative transcription factors, and lineage plasticity[14,15]. Identifying supplementary signaling pathways that influence CRPC progression may enhance the formulation of more efficacious therapeutic medicines, including those aimed at DNA damage repair, the PI3K/AKT/mTOR, and epigenetic modifications[3,16–21]. The growing utilization of combination medications presents optimism for enhanced patient outcomes.

Emerging evidence emphasizes the pivotal functions of RNA m5C epigenetics in cancer biology, encompassing uncontrolled proliferation[22], distant metastasis[23], drug resistance[24,25], immune suppression[26], metabolic plasticity[27], stemness maintain[28], and genomic instability[29]. Nevertheless, two enquiries remain unresolved: (i) the role of RNA m5C alterations in carcinogenesis, and (ii) the regulatory variables governing these m5C methyltransferases. Elucidating these regulatory networks is essential for understanding how RNA m5C epigenetics foster malignant transformation, promotes the distant spread of tumor cells, and facilitates evasion from immune surveillance and therapeutic selection pressures[30–33]. Recent breakthroughs have revealed that NSUN2 can be activated through direct binding to glucose, augmenting tumorigenesis and anti-PD-L1 resistance. These findings underscore the need for further exploration of NSUN2, as understanding its role could provide novel insights into tumor biology and identify new therapeutic targets.

[1]Department of Urology, Fudan University Shanghai Cancer Center, Shanghai, China. [2]Department of Oncology, Shanghai Medical College, Fudan University, Shanghai, China. [3]Department of Urology, Gongli Hospital of Shanghai Pudong New Area, Shanghai, China. [4]Department of Urology, First People's Hospital of Kashi, Kashi, China. [5]Tianjin Medical University, Tianjin, China. [6]These authors contributed equally: Zhenda Wang, Abudurexiti Mierxiati. ✉e-mail: fmmult@foxmail.com; norman.xu@hotmail.com; fnwan06@fudan.edu.cn; dingwei_ye@fudan.edu.cn

Large-scale genome sequencing studies indicate that mutations in FOXA1 are common in prostate cancer, particularly among Chinese patients, and may act as drivers of the disease[34–37]. FOXA1 influences tumor progression in multiple aspects, including malignant transformation, drug resistance, metastasis, and an immunosuppressive microenvironment[38–41]. Traditionally, FOXA1 is associated with defining tissue-specific enhancers and reprogramming AR transcriptional networks[42,43]. However, it also exerts effects independent of AR, involving epithelial-mesenchymal transition (EMT), castration resistance, immune suppression, and neuroendocrine prostate cancer transformation[39,44–46]. Directly targeting FOXA1 for therapeutic purposes faces significant challenges, making it crucial to understand its regulatory network[47–50].

TRIM28 is a protein with complex function, such as ubiquitin E3 ligase[51], epigenetic modulator[52], transcriptional activator[53]. It was involved in complex biological processes in many cancers, including immune surveillance evasion[54–56], replicative immortality[53], tumorigenesis[51], cancer metastasis[57]. In prostate cancer, there are few studies on TRIM28, involving in AR signaling pathway[58], plasticity of luminal cells[59], and degradation of p-Rb[60]. These results implied that TRIM28 can promote tumorigenesis in many ways.

This study screened for a series of m5C methyltransferases, identifying NSUN2 as a factor linked to poor prognosis in PRAD. Our findings show that, in CRPC models, ectopic NSUN2 expression dramatically increases cell proliferation, tumor development, and metastasis. We additionally validated TRIM28 to be a subsequent target of NSUN2, demonstrating that NSUN2 stabilizes TRIM28 mRNA in a m5C-dependent manner, as identified by YBX1. Additionally, we identified FOXA1 as an upstream regulator that upregulates NSUN2 expression. This research provides compelling evidence that, in CRPC, the FOXA1-NSUN2-TRIM28 axis serves as a predictive biomarker and therapeutic target, emphasizing NSUN2's role in this context.

Results

Integrated multi-databases analysis to identify NSUN2 as a target of PRAD

To uncover the roles of m5C modification, we analyzed m5C writers' expression, including DNMT2, NOP2, NSUN2, NSUN3, NSUN4, NSUN5, NSUN6, NSUN7, using the TCGA and GSE46602 databases. Our analysis revealed that NOP2, NSUN2, NSUN3, and NSUN7 exhibited elevated expression in cancer tissues in the TCGA dataset, while DNMT2 (also known as TRDMT1) showed decreased expression (Fig. 1A). In the GSE46602 dataset, DNMT2, NOP2, NSUN2, NSUN3, and NSUN7 also demonstrated increased expression, whereas NSUN6 showed decreased expression (Fig. 1B).

We then assessed Disease-Free Survival (DFS) (Supplementary Fig. 1A), finding significant differences only for NSUN2 and NSUN5 among the various groups. Given our focus on cancer pathogenesis, NSUN2 emerged as a potential target. Notably, NSUN2 mRNA expression was higher in cancer tissues across both TCGA (Supplementary Fig. 1B) and was associated with lymph node metastasis (Supplementary Fig. 1C) and TP53 mutation status (Supplementary Fig. 1D). Furthermore, a substantial correlation between NSUN2 expression and disease-specific survival (DSS) and progression-free interval (PFI) was found using uniCox regression analysis (Fig. 1C, D). Increased NSUN2 expression was significantly correlated with prostate carcinoma and linked to a worse prognosis. We analyzed public database records to investigate the expression changes of m5C methyltransferases before and after castration (Fig. 1E). Among these enzymes, NSUN2 showed an initial decrease followed by an increase post-castration (Fig. 1F), indicating its potential involvement in the development of resistance to ADT over time. Through exploring public databases, we found that many genes mutation before and after ADT. Notably, genes such as FOXA1 and AR exhibited extensive amplification (Fig. 1G).

In CRPC, cancer cells migrate and proliferat more quickly when NSUN2 is present

To evaluate NSUN2 function, we enriched pathways activated in prostate cancer with high NSUN2 expression, including androgen response, oxidative phosphorylation, unfolded protein response, and mitotic checkpoint (Supplementary Fig. 1H). We conducted several experiments, including CCK-8, colony formation, scratch, and Transwell assays. We established NSUN2 knockdown and overexpression cell lines in C4-2 (Fig. 2A) and 22Rv1 (Fig. 2B), confirming efficiency via Western blot and RT-qPCR. Inhibition of NSUN2 expression slowed proliferation rates, while increased NSUN2 expression accelerated growth in both C4-2 and 22Rv1 (Fig. 2C, D for C4-2; Fig. 2E, F for 22Rv1). Consistent results were observed in colony formation assays for both C4-2 and 22Rv1 (Fig. 2I, J). We assessed metastatic potential using scratch and Transwell assays, finding a significant decrease in migration ability in C4-2 (Fig. 2G) and 22Rv1 (Fig. 2H, K) cells upon NSUN2 suppression. Conversely, NSUN2 overexpression enhanced migration in 22Rv1 cells (Fig. 2H, K). The findings demonstrate that NSUN2 stimulates CRPC growth and metastasis. By subcutaneously injecting BALB/cA nude mice, we created a tumor-bearing model to study NSUN2 function in the carcinogenesis of CRPC in vivo. Extracted tumors are depicted in Fig. 2L. Comparing the shNSUN2 group to the negative control (NC) group, an analysis of subcutaneous tumor tissues showed considerably smaller and less massy tumors, whereas the NSUN2-oe group had larger tumors than the NC group (Fig. 2M, N). Immunohistochemical staining showed a decrease in NSUN2, TRIM28, and Ki67 abundance following NSUN2 attenuation (Fig. 2O).

FOXA1 regulates NSUN2 expression by directly binding to its promoter

To identify transcription factors associated with elevated NSUN2 expression, we designed a screening schematic (Fig. 3A). We selected transcription factors linked to androgen receptor (AR)-dependent prostate cancer(ARPC) from single-cell prostate cancer atlas data through differential gene analysis. We then compared expression correlations between NSUN2 and these transcription factors across three prostate cancer datasets, filtering out factors with p-values exceeding 0.05, resulting in a heatmap (Fig. 3B). Six transcription factors (FOXA1, AFF3, TFAP2C, ZMIZ1, ZNF217, ZNF649) showed consistent correlations. Among these factors, FOXA1, recognized as a pioneer lineage-specific TF in prostate cancer[42], exhibited a constantly stronger correlation[38,39]. Using three datasets and TCGA, we verified the positive correlation between NSUN2 and FOXA1 expression (Fig. 3C, D, E, H). Additionally, we assessed FOXA1 and NSUN2 levels in PCa cells and normal epithelial cells via Western blot (Fig. 3F, Supplementary Fig. 2E) and qPCR (Fig. 3G, Supplementary Fig. 2F). In C4-2 (Fig. 3I, J) and 22Rv1 (Fig. 3K, L) cells, we examined NSUN2 expression following FOXA1 knockdown or overexpression. Silencing FOXA1 resulted in decreased NSUN2 expression, while its overexpression led to increased NSUN2 levels. To further investigate chromatin state transitions indicating transcription program activation, we investigated chromatin accessibility in the NSUN2 promoter, which is characterized as 1000 bp upstream of the transcription start site. Chromatin accessibility was characterized using ChIP-Seq for H3K27Ac and H3K4me3, along with ATAC-Seq (Fig. 4A). Scanning for FOXA1 binding sites in this region identified two motifs using JASPAR (http://jaspar.genereg.net/) (Fig. 4B)[61]. ChIP-qPCR assays demonstrated increased binding signals of FOXA1 in the NSUN2 promoter (Fig. 4C, D). Luciferase reporter plasmids were constructed to include the promoter region. Following FOXA1 co-transfection, Dual-Luciferase reporter assays indicated that FOXA1 binds to the −250 to 0 bp region of the NSUN2 promoter (Fig. 4E). We also created mutated luciferase reporter plasmids, including deletions and mutations of the binding sites (Fig. 4F, G). Luciferase assays confirmed that these mutations blocked FOXA1-induced transcriptional upregulation. Subsequently, we suppressed NSUN2 expression in cells overexpressing FOXA1 (Fig. 4H). CCK-8 assay (Fig. 4I) and colony formation assay (Fig. 4J) illustrated that the tumorigenic effect of FOXA1 was reduced following NSUN2 knockdown. These results confirm that FOXA1 transcriptionally activates NSUN2 expression, thereby enabling NSUN2 to function as an oncogene (Fig. 3M).

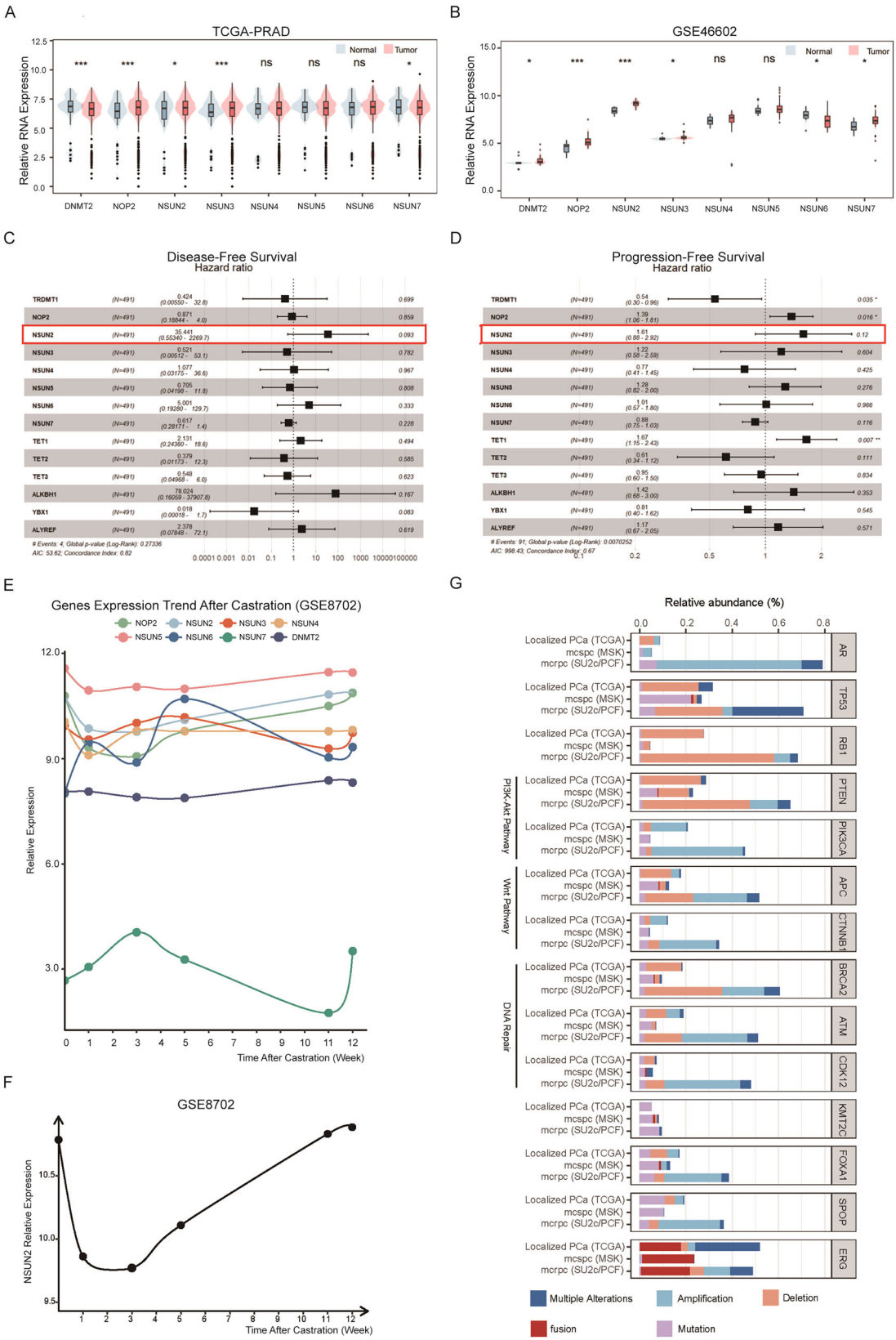

Fig. 1 | Bioinformatics analysis reveals NSUN2 as an oncogene in prostate cancer. **A**, **B** Relative expression of m5C "Writers" in prostate cancer (PRAD) tissues, as analyzed from the TCGA (**A**) and GSE46602 (**B**) databases. **C**, **D** Forest plots displaying univariate Cox regression analyses for Disease-Free Survival(DFS) (**C**) and Progression-Free Survival(PFS) (**D**), adjusted for m5C regulators in PRAD. The plots show hazard ratios along with their 95% confidence intervals. **E** Changes in the expression of m5C methyltransferases following castration. The relative expression levels of gene mRNA are derived from GSE8702. **F** Temporal changes in the NSUN2 expression levels in prostate cancer post-castration. The relative expression levels of gene mRNA are derived from GSE8702. **G** Variability in the mutation status of hotspot genes across different stages. The gene mutation data is sourced from the TCGA, MSKCC, and SU2C projects.

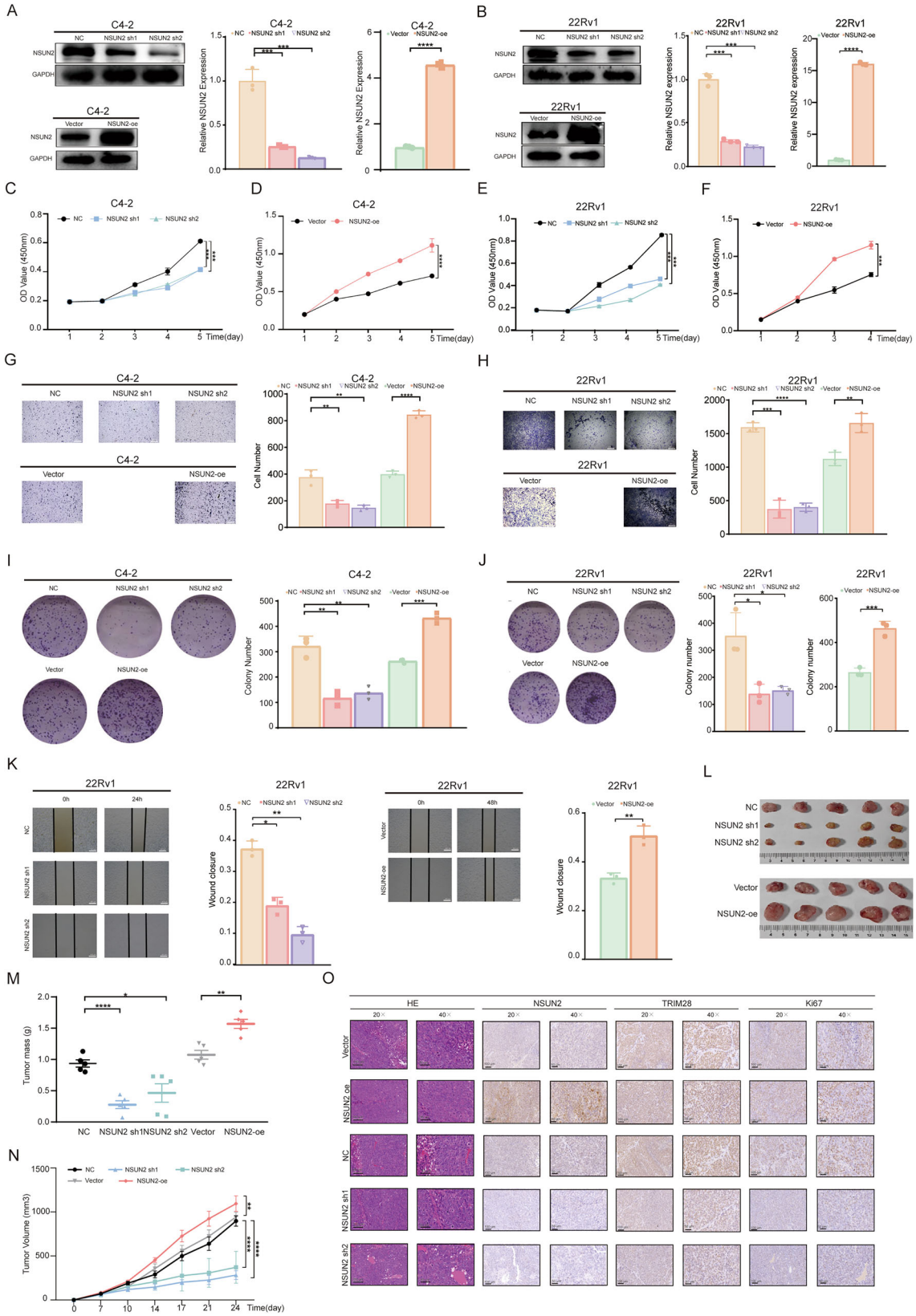

NSUN2 promotes TRIM28 expression in CRPC

We hypothesized that NSUN2 facilitates prostate cancer proliferation and metastasis through its activity as a methyltransferase. To test this, we conducted transcriptomic sequencing on C4-2 cells overexpressing NSUN2. The downstream gene screening proceeded as follows: initially, 68 genes were identified by integrating bisulfite sequencing data from an established C4-2R cell line[62] and clinical specimens from prostate cancer patients before and after abiraterone treatment, sourced from FUSCC. Cross-referencing with a proto-oncogene database further refined the list to eight genes (MARCKS, TRIM28, PRKCD, NAAA, DDX6, ARAF, HSPB1, JUN).

Fig. 2 | NSUN2 promotes cancer cells proliferation and migration in PRAD. **A**, **B** Representative immunoblotting assays and qPCR analyses demonstrate the efficiency of transfection in C4-2 (**A**) and 22Rv1 (**B**) cell lines. **C**, **D** Quantification results from the CCK-8 proliferation assay showing the effects of NSUN2 knockdown (**C**) and overexpression (**D**) in C4-2 cells. **E**, **F** Quantification of the CCK-8 proliferation assay for 22Rv1 cells, illustrating the effects of NSUN2 knockdown (**E**) and overexpression (**F**). **G**, **H** Representative images and quantification of invasion assays in NSUN2-knockdown, NSUN2-overexpressing, and control C4-2 (**G**) or 22Rv1 (**H**) cells. Scale bar = 400 μm. Quantification data is also provided. **I**, **J** Representative images of the colony formation assay in C4-2 (**I**) and 22Rv1 (**J**) cells, with corresponding quantification data. **K** Representative images and quantification of migration assays for NSUN2-knockdown, NSUN2-overexpressing, and control 22Rv1 cells. Scale bar: 400 μm. Quantification data is also provided. **L** Tumor images from nude mice implanted with parental, NSUN2 knockdown, or overexpressing 22Rv1 cells ($n = 5$). **M**, **N** Tumor mass (**M**) and growth curves (**N**) for implanted tumors formed by parental, NSUN2 knockdown, or overexpressing 22Rv1 cells. **O** Representative HE staining and IHC images showing NSUN2, TRIM28, and Ki67 staining in implanted tumors from NSUN2 knockdown or overexpressing cells. 20×: Scale bar = 100 μm, 40×: Scale bar = 50 μm.

Ultimately, TRIM28 was selected as the key downstream target gene (Fig. 5A).

Increased TRIM28 expression in the TCGA database correlated with poorer prognosis. (Fig. 5D, E), and there was a notable positive association found between NSUN2 and TRIM28 expressions (Fig. 5B, C). To investigate the regulation of TRIM28 by NSUN2, we performed qRT-PCR and western blot, confirming that NSUN2 knockdown led to downregulation of TRIM28 in mRNA and protein levels (Fig. 5F, G, Supplementary Fig. 2A, B). Given that FOXA1 positively regulates NSUN2, we explored whether FOXA1 could regulate TRIM28 via NSUN2. Stable cell lines with FOXA1 knockdown or overexpression demonstrated that TRIM28 expression was inhibited by FOXA1 silencing and increased with FOXA1 overexpression (Fig. 5H, I, Supplementary Fig. 2C, D). Additionally, CRPC cell lines (C4-2, C4-2B, and 22Rv1) showed a strong positive connection in the expression of FOXA1, NSUN2, and TRIM28 (Supplementary Fig. 2E, F).

We further hypothesized that NSUN2 promotes TRIM28 expression through an m5C-dependent mechanism. To test this, we conducted RIP, RNA pulldown, and RNA stability assay. RIP indicated that the anti-NSUN2 antibody significantly enriched TRIM28 mRNA, supporting NSUN2's role in targeting TRIM28 for m5C modification (Fig. 5J). The m5C-specific antibody further enriched TRIM28 mRNA in NSUN2-overexpressing cells, compared to NSUN2 knockdown cells (Fig. 5K). Bisulfite sequencing identified potential methylation sites (Fig. 5L), and RNA pulldown assays using biotin-labeled probes confirmed seven NSUN2-bound sites on TRIM28 mRNA (Fig. 5M).

TRIM28 promotes cancer cell proliferation and migration in CRPC

To further understand TRIM28's role in CRPC, bioinformatics analysis of published databases revealed its involvement in post-translational modifications, alternative splicing regulation, cell cycle, and cell motility (Fig. 6A, Supplementary Fig. 3A). In vitro assays with two distinct shRNAs targeting TRIM28 confirmed knockdown efficiency via qRT-PCR and western blot (Fig. 6B, G, Supplementary Fig. 3B). TRIM28 inhibition significantly suppressed proliferation, as demonstrated by CCK-8 assays, while overexpression promoted proliferation (Fig. 6C, D, H, I). Similar results were observed in colony formation assays (Fig. 6E, J, Supplementary Fig. 3C). Migration assays, including wound healing and Transwell, showed that TRIM28 downregulation hindered migration, while upregulation enhanced it (Fig. 6F, K, L Supplementary Fig. 3D, E).

TRIM28 mRNA's m5C alteration, mediated by NSUN2, preserves its YBX1-dependent stability

Next, we identified the "Reader" protein that binds to the m5C modification sites on TRIM28 mRNA. From public databases, we predicted that YBX1 and ALYREF, well-known m5C readers, showed the highest correlation with TRIM28 mRNA expression (Fig. 7A). TRIM28 expression was decreased when YBX1 was silenced (Fig. 7B, C), suggesting its role in stabilizing TRIM28 mRNA. RIP assays confirmed direct interaction between YBX1 and TRIM28 mRNA (Fig. 7D). Moreover, in vitro experiments demonstrated that YBX1 promotes prostate cancer proliferation and metastasis (Supplementary Fig. 3F, G).

Since RNA stability is commonly regulated by methylation, we observed that NSUN2 knockdown dramatically suppressed the stability of TRIM28 mRNA in cells with the transcription inhibitor Act D (Fig. 7E, F). Given that FOXA1 regulates TRIM28 through NSUN2, we further examined the impact of FOXA1 on TRIM28 mRNA stability. TRIM28 mRNA was destabilized upon FOXA1 knockdown (Fig. 7G, H), and FOXA1-induced RNA stability was attenuated when NSUN2 was silenced (Fig. 7I). Finally, we silenced TRIM28 in NSUN2-overexpressing cells and found that TRIM28 knockdown markedly suppressed NSUN2-induced CRPC growth (Fig. 7J, K, L).

NSUN2 has a higher expression in PRAD with a worse prognosis

In the prostate cancer samples, a favorable connection was seen between elevated Gleason Scores and heightened NSUN2 expression (Supplementary Fig. 1E). Similarly, TRIM28 expression followed this trend (Supplementary Fig. 1F). Immunohistochemistry (IHC) further demonstrated significantly elevated NSUN2 levels in prostate cancer tissues (Supplementary Fig. 1G).

Discussion

Cancer is a primary disease threatening human health[63–65]. Prostate cancer remains a significant global health burden, with thousands of new cases reported annually[66]. While ADT has achieved notable success in managing prostate cancer, resistance to this treatment often arises within two to three years, triggering CRPC[67]. Although clinical signs of CRPC manifest over a period of two to three years, molecular alterations begin as early as three months post-therapy[68]. The causes of metastatic CRPC are multifaceted[56,69–74], involving mechanisms such as restoration of androgen receptor (AR) transcription programs and lineage plasticity. The restoration of AR activity occurs through AR splice variants, AR mutations, or AR amplification. Lineage plasticity, by which cancer cells change their identities to elude selection pressure brought by drugs, involves a complex set of molecular events. Epigenetic analysis of prostate cancer patients undergoing 3 months of neoadjuvant enzalutamide monotherapy revealed that FOXA1 rewires cis-regulatory elements in an AR-independent manner to activate proliferative signals, including those mediated by ARNTL[68]. Research on the mechanisms underlying CRPC is essential for understanding the disease's pathophysiology and for identifying new therapeutic targets.

Although RNA methylation has been increasingly acknowledged as a critical factor in tumorigenesis, most studies have concentrated on N6-methyladenosine (m6A) modification[75–80]. Conversely, 5-methylcytosine (m5C), a second RNA methylation modification, has not received as extensive investigation. To identify potential targets involved in m5C modification, we constructed a geneset of methyl-transferases, identifying NSUN2 as a candidate by integrating gene expression data with prognostic information. Recent studies have highlighted NSUN2's role across cancers, including gastric cancer[81], esophageal squamous cell carcinoma[82,83], pancreatic cancer[84], hepatocellular carcinoma[85], bladder cancer[86]. Notably, NSUN2 plays roles in biological processes such as RNA methylation and mRNA stabilization. It was recently discovered that glucose functions as a cofactor, facilitating the activation of NSUN2. This process preserves m5C RNA methylation globally and stabilizes TREX2, leading to tumorigenesis and failure of anti-PD-L1 immunotherapy[87]. However, the specific mRNAs modified by NSUN2 in prostate cancer remain unclear. According to a bioinformatics analysis, prostate cancer patients exhibiting elevated NSUN2 expression levels demonstrate a poorer prognosis[88]. Despite this, NSUN2's

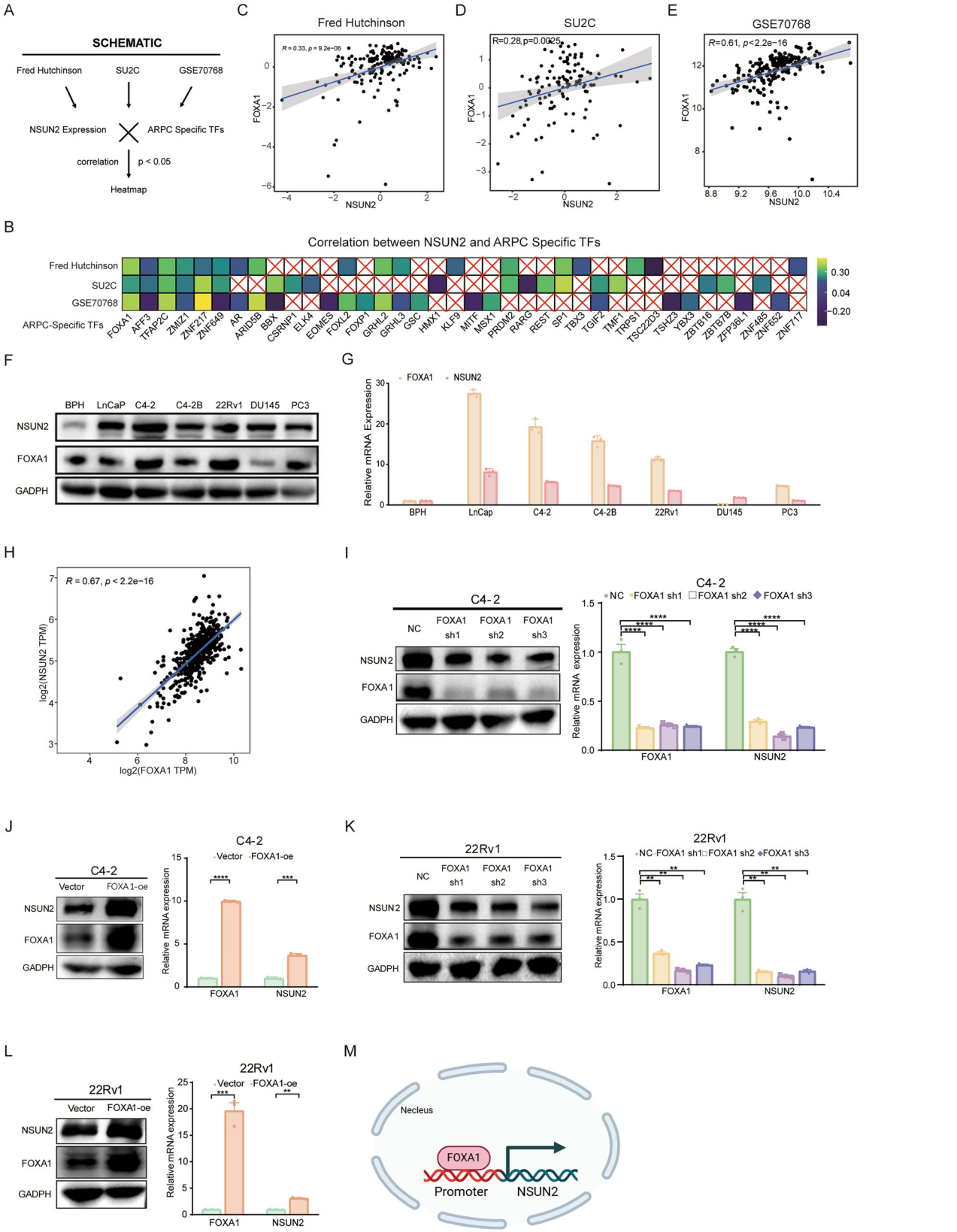

Fig. 3 | Cross-validation confirms a high positive correlation between NSUN2 and FOXA1 expression. **A** Schematic representation of the screening process for transcription factors associated with high expression levels of NSUN2. **B** Correlation analysis of AR-specific transcription factors with NSUN2 expression in the Fred Hutchinson, SU2C, and GSE70768 datasets. A cross within the box indicates that the correlation is not statistically significant. **C**–**E** Correlation analysis between FOXA1 and NSUN2 expression in the Fred Hutchinson (**C**), SU2C (**D**), and GSE70768 (**E**) datasets. **F**, **G** Representative immunoblotting assay (**F**) and qPCR analysis (**G**) demonstrating the expression of FOXA1 and NSUN2 in normal and cancerous cell lines. **H** Correlation between FOXA1 and NSUN2 expression in the TCGA database for prostate adenocarcinoma (PRAD). **I**, **J** Representative immunoblotting assays and qPCR results showing the expression levels of NSUN2 following FOXA1 knockdown (**I**) and overexpression (**J**) in C4-2 cells. **K**, **L** Representative immunoblotting assays and qPCR results illustrating the expression levels of NSUN2 after FOXA1 knockdown (**K**) and overexpression (**L**) in 22Rv1 cells. **M** Graphical abstract summarizing the mechanism by which FOXA1 regulates NSUN2 expression.

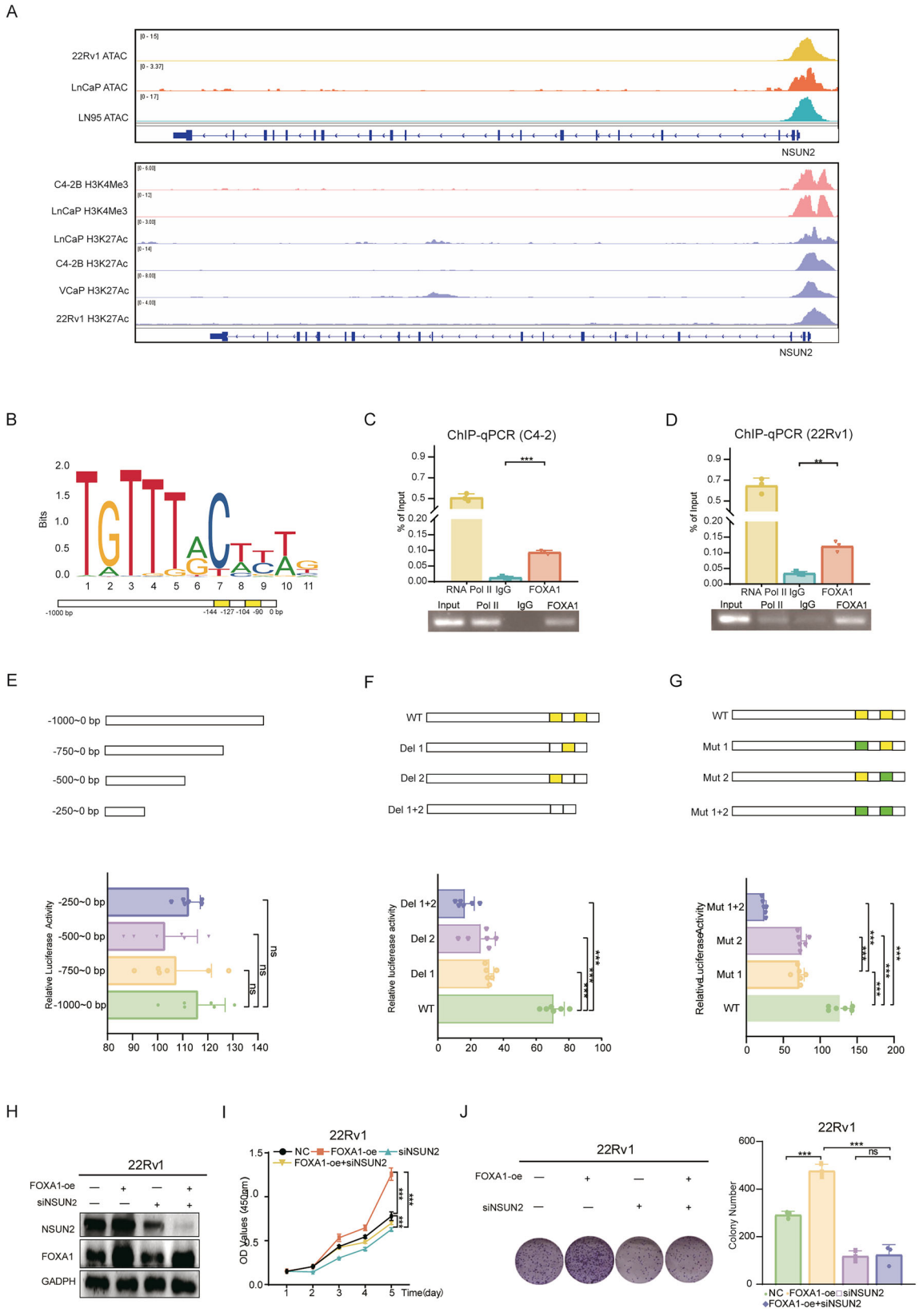

role in PCa and its potential regulatory mechanisms have not been elucidated. In this study, we validated NSUN2's role in CRPC using C4-2 and 22Rv1 cell lines, both of which are representative models of CRPC. Our results showed that, in CRPC, NSUN2 strengthens proliferation and migration in vitro, consistent with findings from other cancer types[22,26,89,90].

We next investigated the cause of elevated NSUN2 expression. Since transcriptional regulation is a primary driver of gene expression, we searched for transcription factors associated with NSUN2 expression in prostate cancer using public databases. A strong association was identified between NSUN2 expression and FOXA1, a transcription factor known to assist AR

Fig. 4 | FOXA1 transcriptionally activates NSUN2 expression by attaching to NSUN2 promoter. A Chromatin accessibility and the binding sites of FOXA1. **B** Identification of two FOXA1 consensus binding sites located within the −1000 to 0 bp region of the NSUN2 promoter. **C**, **D** Chromatin immunoprecipitation (ChIP) assays conducted in C4-2 (**C**) and 22Rv1 (**D**) cell lines using anti-FOXA1. Results indicate that FOXA1 binds to NSUN2 promoter. **E**–**G** Identification of FOXA1 response elements within the noncoding region of NSUN2. The regions within the 1000 bp proximal promoter of the NSUN2 gene were analyzed using distinct promoter-luciferase reporter constructs. Luciferase activity was analyzed in HEK293T cells transfected with FOXA1 for a duration of 48 h. Luciferase activity analysis in HEK293T cells. Cells were transfected with either the wild-type NSUN2 promoter-luciferase reporter (WT) or truncation (**E**), various mutant reporters (**G**) and deletion constructs (**F**) alongside FOXA1 for 36-48 h. **H** Representative immunoblotting assay assessing the expression levels of FOXA1 and NSUN2 following FOXA1 overexpression after NSUN2 knockdown. **I** Quantification of CCK-8 proliferation assay results following FOXA1 overexpression after NSUN2 knockdown. **J** Representative images from the colony formation assay after FOXA1 overexpression following NSUN2 knockdown, along with corresponding quantification data.

in binding target genes and driving prostate cancer progression[35–37,91]. FOXA1 mutations, frequently observed in prostate cancer, are linked to the malignant phenotype[92]. However, extensive study has demonstrated that FOXA1 can function in an AR-independent manner[91]. EMT is inhibited by FOXA1 in a way that is independent of AR[39]. Immunological response to malignancy, interferon signaling gene expression, and STAT2 DNA-binding activity were all inhibited by FOXA1's interaction with the STAT2 DNA-binding domain[93]. FOXA1 has also been reported to repress NR3C1 (glucocorticoid receptor gene) via the corepressor TLE3[94]. These findings suggest that FOXA1's full spectrum of functions is still not fully understood. We demonstrated that FOXA1 regulates NSUN2 expression through transcriptional control, as confirmed by ChIP and luciferase assay.

Through the integration of RNA-seq data and bisulfite sequencing, TRIM28 was discovered as a downstream target of NSUN2. TRIM28 is a versatile protein implicated in numerous biological processes, including tumorigenesis[51], cell proliferation[34], metastasis[95], antitumor immunity[38,54,55,96], and drug resistance[97,98]. It has at least three aspects of function: first, as a RING-type ubiquitin E3 ligase, it can catalyze the ubiquitination and degradation of protein kinases such as AMPK[99]. Secondly, as a SUMOylation E3 ligase, it promotes the SUMOylation of PD-L1[100]. Thirdly, as a scaffold protein, It attaches to several chromatin remodeling complexes on chromosomes to inhibit transcription[101]. These functions are extensively involved in processes such as tumor drug resistance[102] and tumor immunity[100]. The TCGA data indicates that TRIM28 exhibits abnormal expression in numerous cancer types. The role of TRIM28 shows considerable variation across different cancer types. In prostate cancer and other cancers, TRIM28 can act as an oncogenic factor, while in renal cell carcinoma, the anti-tumorigenic effect of TRIM28 is quite evident. In some tumors, function of TRIM28 is still unclear. In PCa, particularly in CRPC, TRIM28 expression is upregulated, and inhibiting TRIM28 will suppress tumor growth. Mechanistically, TRIM28 activates AR signaling pathway[103], activating proximal luminal lineage cell markers[59]. TRIM28 can also promote prostate cancer pathology process by polyubiquitination and degradation of phosphorylated retinoblastoma protein (p-Rb)[100]. The expression of TRIM28 is also considered a potential stratification factor, and the expression of TRIM28 can be used to predict sensitivity to radiology therapy[104] or chemotherapy[105]. Given TRIM28's influence on the tumor microenvironment, TRIM28 expression interference can significantly increase the efficacy of tumor immunotherapy[106].

Stable transfection cell lines were established with TRIM28 knockdown and overexpression. In vitro assay demonstrates that it facilitates prostate cancer proliferation and metastasis. The regulatory link between NSUN2 and TRIM28 was also confirmed in NSUN2 knockdown and overexpression cells. We hypothesized that TRIM28 is dependent on NSUN2-mediated methylation. The hypothesis was initially supported by the RIP assay. Based on bisulfite sequencing, seven sites were discovered using the RNA Pulldown. These findings illustrated how NSUN2 regulates the TRIM28 expression. Act D is a transcription inhibitor that is frequently used to stop the synthesis of fresh mRNA in mRNA stability assay. As a result, the amount of mRNA that remains after transcription inhibition can be used to evaluate the degradation of mRNA[60]. We then figured out that the m5C modification on TRIM28 mRNA improves its stability using Act D to block the transcription.

RNA methylation modifications typically involve three types of enzymes: "Writers", "Erasers", and "Readers". It is the Writers' responsibility to add methyl groups to RNA. Erasers remove them. Readers recognize and mediate biological responses to methylated RNA. YBX1 and ALYREF are well-known m5C Readers, but additional Readers such as FRPM[29], SRSF2[107], YBX2[108], YTHDF2[109], RAD50[110], have been identified. Previous observations in the literature indicate that distinct Readers appear to affect RNA in different ways. These effects could be attributed to the Reader's own function or to proteins that co-localize with the Reader. For instance, plenty of research indicates that YBX1 affects the stability of mRNA to change its half-life, which in turn impacts the target protein's production[25]. ALYREF, on the other hand, is considered in many studies to change the intracellular distribution of mRNA[111]. It was recently found that the leukemia-associated SRSF2 P95H mutation changed its capacity to read m5C in RNA, resulting in aberrantly spliced mRNA and linked to a poor prognosis in leukemia[107]. FRMP promotes demethylation by TET1 and R-loop unwinding to facilitate DNA repair by recognizing m5C sites on mRNA[29]. YTHDF2 is involved in pre-rRNA processing in cells by binding directly to m5C in rRNA[109]. Therefore, we believe that YBX1 or ALYREF is more likely to be the Reader that recognizes TRIM28 mRNA, which means that both of them show a significantly positive correlation with TRIM28 mRNA.

We then examined the relationship between different Readers and the expression of TRIM28 mRNA across several available databases. It was found that YBX1 and ALYREF are the most robust Readers. We knocked down YBX1 and ALYREF in CRPC cell lines and confirmed their impact on TRIM28 expression. RIP assays further validated the binding of YBX1 to TRIM28 mRNA, reinforcing the hypothesis that NSUN2-mediated methylation enhances TRIM28 mRNA stability via YBX1. These results reveal a new signaling axis: FOXA1-NSUN2-TRIM28, and construct a regulatory network centered on RNA epigenetics, where multiple biological processes engage in crosstalk with each other.

However, this study has some limitations. First, previous studies have reached controversial conclusions regarding the role of FOXA1 in CRPC metastasis. This study did not address whether the promotion of tumor metastasis by TRIM28 is caused by overexpression of FOXA1, and this issue requires further research. Secondly, further proof is required to validate TRIM28's role in NSUN2's stimulation of tumor growth and metastasis. Thirdly, there is a lack of more preclinical models (patient-derived organoids, patient-derived xenografts, etc.) to evaluate the clinical prospects of targeting the FOXA1-NSUN2-TRIM28 axis.

In conclusion, this study demonstrates that NSUN2 adds m5C methylation marks to TRIM28 mRNA, which are recognized by YBX1 to maintain TRIM28 mRNA stability. This, in turn, promotes CRPC proliferation and metastasis. Additionally, FOXA1, a lineage-specific transcription factor, regulates NSUN2 expression, highlighting the complex regulatory mechanisms. Given TRIM28's extensive involvement in cancer biology, our findings suggest that targeting the FOXA1-NSUN2-TRIM28 axis could serve as a promising therapeutic approach for PCa, particularly CRPC.

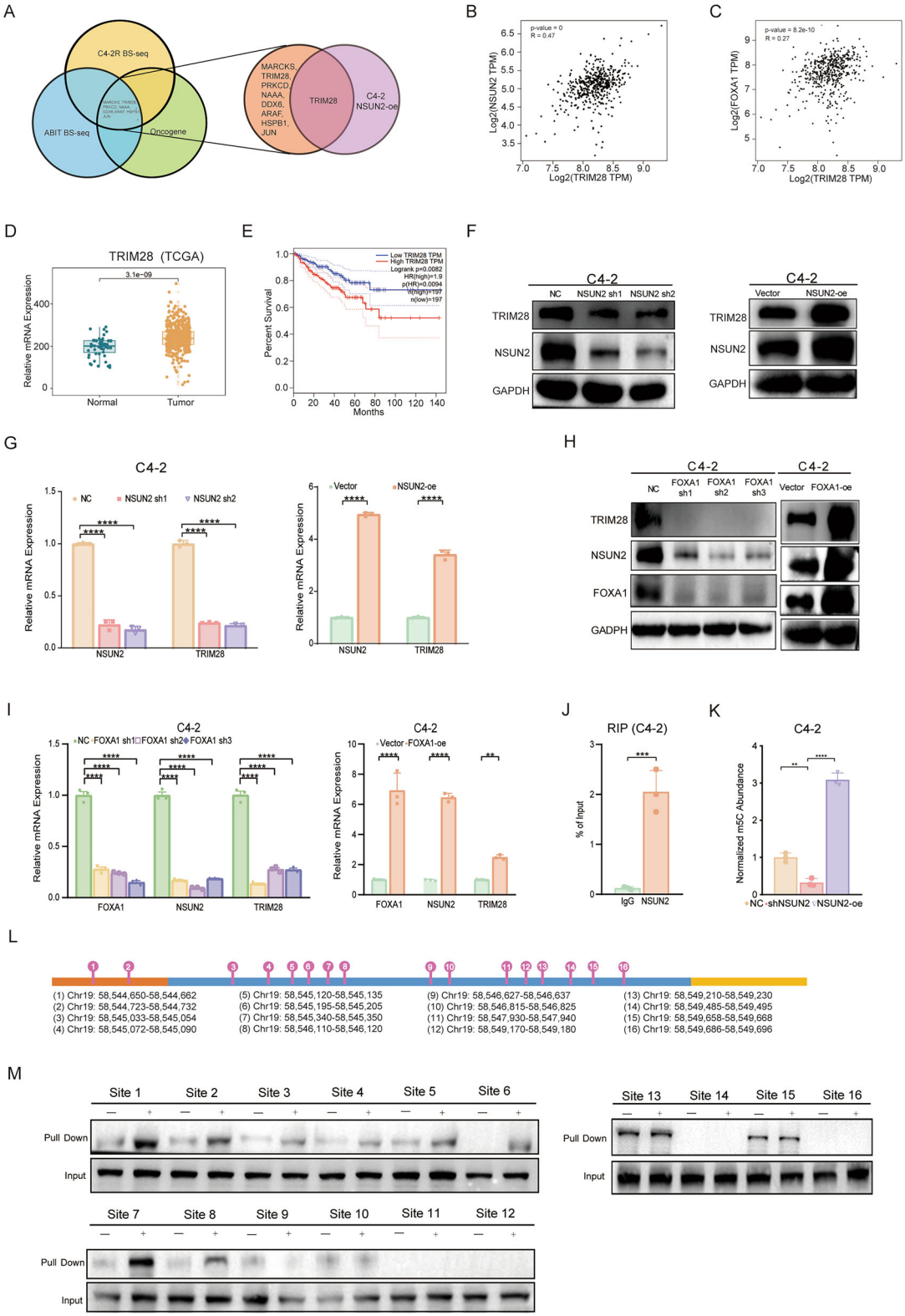

Fig. 5 | NSUN2 promotes the TRIM28 expression by adding m5C modification to TRIM28 mRNA. A Identification of TRIM28 as a downstream target regulated by NSUN2. **B** Correlation analysis between NSUN2 and TRIM28 expression using the TCGA database for prostate cancer (PRAD). **C** Correlation analysis between FOXA1 and TRIM28 expression using the TCGA cohort for PRAD. **D** Relative expression levels of TRIM28 in PRAD compared to tumor-adjacent tissues in TCGA. **E** Kaplan-Meier analysis illustrating differences in Disease-Free Survival (DFS) based on TRIM28 expression in prostate cancer (PRAD), analyzed via GEPIA. **F**, **G** Evaluation of TRIM28 expression following NSUN2 knockdown or overexpression in C4-2 cells, demonstrated by representative immunoblotting assays (**F**) and quantitative PCR (**G**). **H**, **I** Assessment of TRIM28 and NSUN2 expression after FOXA1 knockdown or overexpression in C4-2 cells, shown through representative immunoblotting (**H**) and qPCR analysis (**I**). **J** RNA Immunoprecipitation (RIP) assays in C4-2 cells demonstrating the direct binding of NSUN2 protein to TRIM28 mRNA, as measured by qPCR. **K** RIP assays indicating that the m5C abundance of TRIM28 mRNA fluctuates with changes in NSUN2 expression, assessed by qPCR. **L** Graph showing m5C abundance in TRIM28 transcripts utilizing Bisulfite sequencing. **M** Representative immunoblotting results of NSUN2 following RNA Pulldown assays using cell lysate (Ly.) and biotinylated TRIM28 probes.

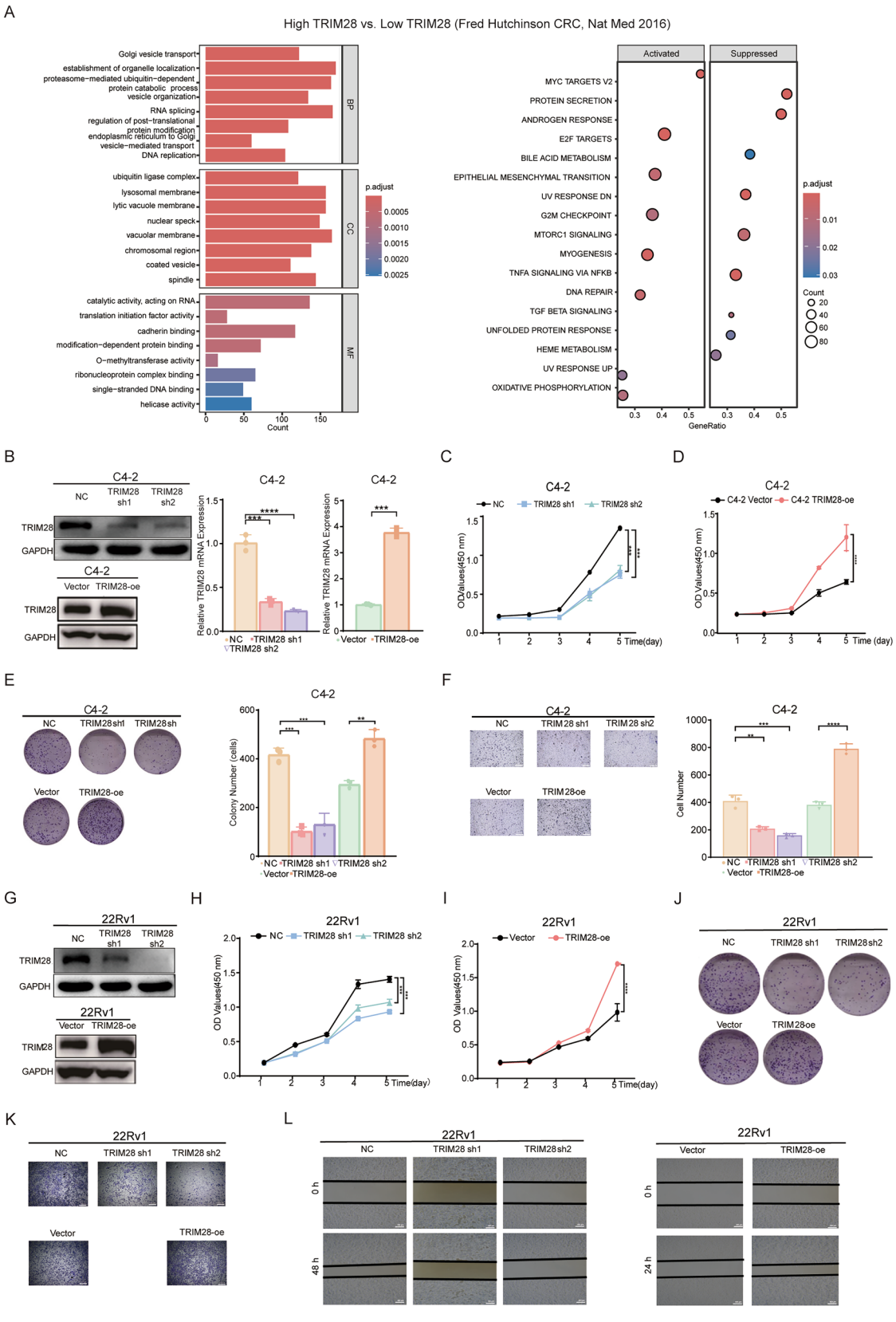

Materials and methods

Ethics statement and immunohistochemistry (IHC)

The study was carried out in strict accordance with the principles enshrined in the Declaration of Helsinki, and was approved by the Medical Ethics Committee of Cancer Hospital, Fudan University (SCCIRB). Prior to the collection of tumor samples, written informed consent was obtained by the patients, and the procedure was executed in compliance with institutional and state laws governing the use of human tissues for experimental purposes. Tumor tissues fixed and embedded underwent deparaffinization, rehydration, and heat-mediated antigen retrieval. After incubation with 3%

Fig. 6 | TRIM28 promotes cancer cells proliferation and migration in vitro. **A** KEGG and GSEA analyses indicate pathways enriched in samples with high TRIM28 expression. **B** Representative immunoblotting assay and quantitative PCR (qPCR) demonstrate the efficiency of TRIM28 knockdown and overexpression in C4-2 cells. Quantification of CCK-8 proliferation assays showing the effects of TRIM28 knockdown (**C**) and overexpression (**D**) in C4-2. **E** Representative images and quantification from the colony formation assay comparing TRIM28 knockdown and overexpression in C4-2. **F** Representative images and quantification of invasion assays for TRIM28-knockdown, TRIM28-overexpression, and control C4-2 cells. Scale bar: 400 μm. **G** Representative immunoblotting assay confirming the efficiency of TRIM28 knockdown and overexpression in 22Rv1 cells. Quantification of CCK-8 proliferation assays in TRIM28 knockdown (**H**) and overexpression (**I**) in 22Rv1 cells, presented as mean ± SD ($n = 6$). **J** Images of colony formation assay in TRIM28 knockdown and overexpression 22Rv1, with corresponding quantification data. **K** Transwell assay results comparing TRIM28 knockdown and overexpression in 22Rv1. Scale bar: 400 μm. **L** Representative images of migrated TRIM28-knockdown, TRIM28-overexpression, and control 22Rv1 cells, with quantification data included. Scale bar: 400 μm.

methanol-H2O2 for 10 min, sections underwent treatment with normal goat serum for a duration of 10 min. and subsequently stained with primary antibodies overnight at 4 °C as follows: NSUN2 (1:600, Proteintech, Cat No. 20854-1-AP), TRIM28 (1:600, Proteintech, Cat No. 15202-1-AP), and Ki-67 (1:800, Cat No. 27309-1-AP, Proteintech). Sections were stained using diaminobenzidine (DAB-2031, Fuzhou Maixin Biotech) after being treated for 30 min with secondary antibodies (Proteintech, Cat. No. PR30011). Pictures were taken with an Olympus camera and the software that came with it.

Xenograft tumor growth

All animal procedures at Fudan University were authorized by the Institutional Animal Care and Use Committe, which were in accordance with pertinent ethical regulations. The study used male BALB/cA nude mice that were 3–4 weeks old[112]. 1×10^7 22Rv1 cells with shNSUN2 or NSUN2 overexpression were injected subcutaneously into the animals' dorsal flank. Tumor size was assessed biweekly. Tumor weight was measured following euthanasia via CO_2 asphyxiation for 5 min, and tumor samples were subsequently harvested for additional research.

Cell culture

The C4-2 and 22Rv1 cell lines were obtained from the American Type Culture Collection (ATCC). Researchers kept cells in RPMI 1640 media at 37 °C and 5% CO_2 (Gibco, Shanghai, China), added with a 10% solution of fetal bovine serum (Gibco, Shanghai, China). To minimize contamination, the media received an addition of 1% penicillin–streptomycin (15-140-122, ThermoFisher Scientific) following manufacturer's guidelines.

Western blotting

Proteins were harvested from C4-2 and 22Rv1 cells. After being subjected to electrophoresis, protein samples were moved onto a PVDF membrane manufactured by Millipore in Shanghai, China. Membranes were blocked and incubated with the diluted primary antibodies to 1000 times their concentration at 4 °C overnight: anti-NSUN2 (Proteintech, 20854-1-AP), anti-FOXA1 (Abcam, ab55178), anti-TRIM28 (Proteintech, 15202-1-AP), anti-YBX1 (Abcam, ab76147) and anti-ALYREF (Proteintech, 16690-1-AP). After being cleaned, membranes were stained with secondary antibodies (goat anti-mouse, 1: 5000, Proteintech, SA00012-1; 1: 3000, Proteintech, goat anti-rabbit, SA00001-2) for one hour at room temperature. Utilizing ECL-plus™ chemiluminescence kits (BD Biosciences, NJ, USA), visualization was achieved.

RNA extraction and real-time quantitative PCR (RT qPCR)

TRIzol reagent (ThermoFisher, Shanghai, China) was employed to extract RNA from cells derived from prostate cancer and subsequently reverse transcribed using MasterMix (TaKaRa, Otsu, Japan). RT qPCR was conducted with GAPDH as an internal control.

Cell counting kit-8 assay (CCK-8)

A thousand cells per well were cultivated in a 96-well plate, with six replicates for each sample. Cell viability was evaluated at designated times (24, 48, 72, 96, till 120 h) by measuring OD value at 450 nm.

Colony-forming assay

A thousand cells per well were cultivated in a plate with six wells and cultivated for 10 days. Staining colonies with crystal violet, they were quantified using ImageJ.

Wound healing

Cells were cultivated into 6-well plates. A wound was induced by abrasion of the cellular layer. Cells were subsequently inoculated in a serum-free medium, and migration was evaluated by measuring the wound area at 0 and 24 h (or 12 h) using ImageJ software.

Transwell assay

Fifty thousand cells were cultivated in the Transwell compartment with 250 μL of medium without serum, whilst the lower compartments provided 850 μL medium fortified with 10% FBS. After an interval, the cells were stained with crystal violet, and ImageJ software was used to calculate their numbers.

Cell transfection

Cells underwent transfection with siRNA utilizing Lipo2000 reagent (ThermoFisher Scientific, Waltham, MA, USA). Each plate was treated with 10 μL of siRNA (sequences: siRNA1: CGGGATCTATAACAACACCAT, siRNA2: CCGTGTGTACTTATCCTGGAT, or non-targeting siRNA) in Opti-MEM for a duration of 25 min. The medium was replaced after a duration of six hours. Cells that were transfected were collected for analysis 48 h after transfection.

Chromatin immunoprecipitation assay (ChIP Assay)

C4-2 or 22Rv1 cells (1 × 10^7) were subjected to crosslinking in 1% formaldehyde for ten min, followed by quenching with glycine[112]. Cells were lysed and subjected to sonication with a Bioruptor Sonicator. Input samples were set aside, while the remaining samples underwent overnight immunoprecipitation at 4 °C using FOXA1 antibodies (ab170933, Abcam). Protein G beads underwent incubation at 4 °C for 3 h. Following washes, immunoprecipitated samples were eluted, and DNA amplification was performed using TB Green (RR096A, Takara).

RNA pulldown assay

Cells in a 100 mm plate underwent lysis with a cell lysis buffer. RNA probes were synthesized by Tsingke and biotinylated, and subsequently bound to Streptavidin Magnetic Beads utilizing RNA Capture Buffer[113]. The beads were incubated with protein samples for a duration of 30 to 60 min at 4 °C. Protein complexes were isolated and purified, followed by elution at 37 °C for Western blot analysis.

RNA immunoprecipitation assay (RIP Assay)

RIP assay is carried out utilizing RIP Kit from Millipore (catalog number 17-700)[114]. C4-2 cells in a 100 mm plate were subjected to lysis using RIP lysis buffer. Input samples were reserved, and protein G magnetic beads were incubated with antibodies for 0.5 h at 25 °C. Following a 3-hour incubation of the cell lysate at 4 °C, RNA was subjected to washing with RIP Wash Buffer, followed by purification and extraction utilizing TRIzol. RNA underwent reverse transcription utilizing PrimeScript™ RT Master Mix (RR036A, Takara). It was subsequently amplified with TB Green (RR096A, Takara).

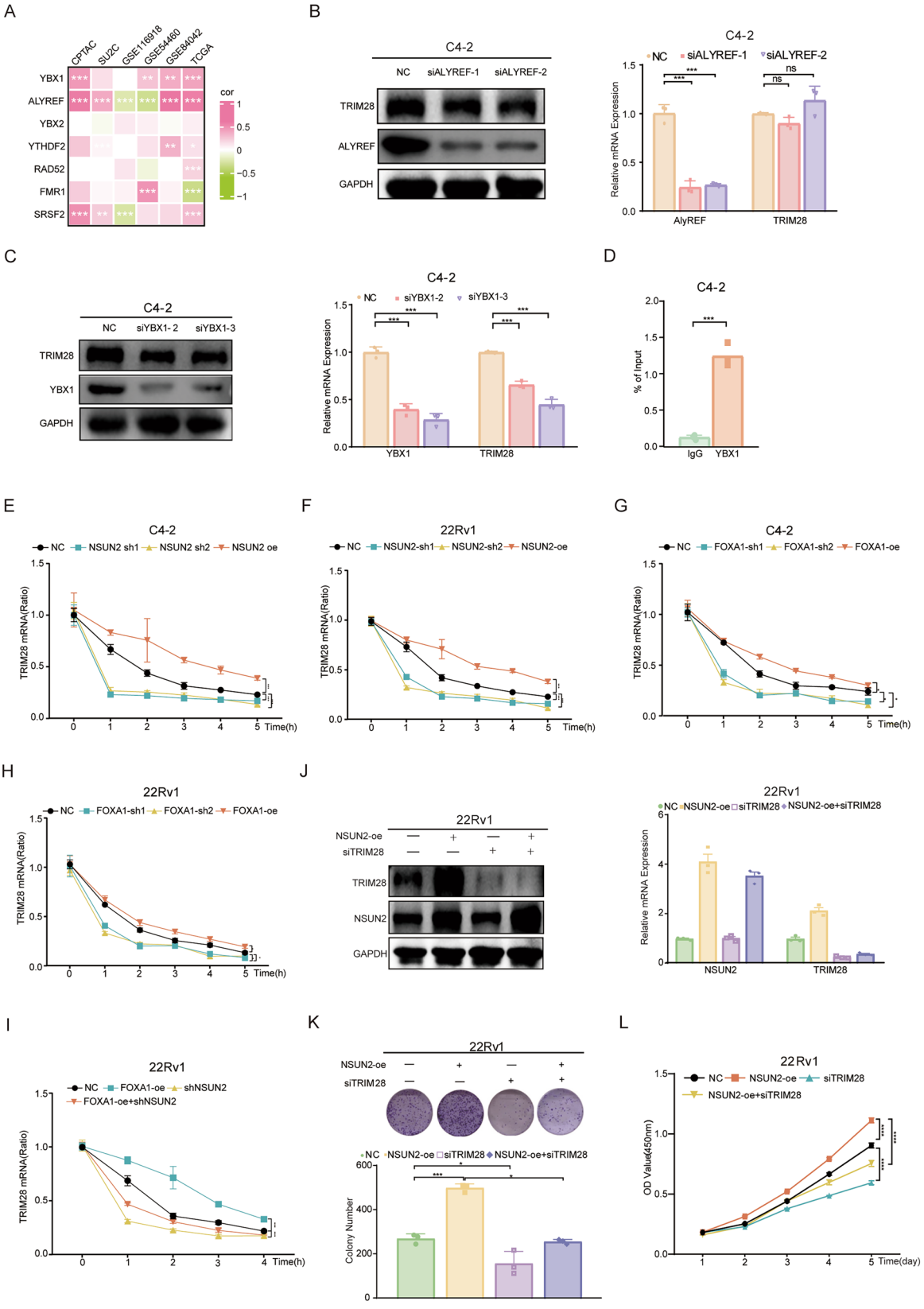

RNA stability assay

The half-life of RNA was measured to evaluate RNA stability[114]. Six replicates were utilized. At some time points (0, 1, 2, 3, 4, and 5 h), 5 μg/mL of Act D (MCE, HY-17559) was given. In order to ascertain the relative quantity of TRIM28 mRNA in relation to the 0-hour time point, RNA was extracted and subjected to RT-qPCR.

Fig. 7 | YBX1, acting as a reader, is involved in maintaining the stability of TRIM28 mRNA mediated by NSUN2 in an m5C-dependent manner. A A heatmap illustrating the correlation between TRIM28 mRNA expression and seven reader proteins. **B**, **C** Representative immunoblotting assay and quantitative PCR (qPCR) showing TRIM28 expression after knocking down ALYREF (**B**) and YBX1 (**C**) in C4-2 cells. **D** RNA immunoprecipitation (RIP) assays in C4-2 cells demonstrating the direct binding between YBX1 protein and TRIM28 mRNA, analyzed by qPCR. **E**, **F** The decay rate of TRIM28 mRNA at designated time intervals following actinomycin D (5 μg/ml) treatment in C4-2 (**E**) and 22Rv1 (**F**) after NSUN2inhibition and overexpression, respectively, measured by qPCR. **G**, **H** The decay rate of TRIM28 mRNA at designated time intervals following actinomycin D (5 μg/ml) treatment in C4-2 (**G**) and 22Rv1 (**H**) following FOXA1 inhibition and overexpression, analyzed by qPCR. **I** The decay rate of TRIM28 mRNA at designated time intervals following actinomycin D (5 μg/ml) treatment in 22Rv1 NSUN2 knockdown cells, with or without FOXA1 overexpression, assessed by qPCR. **J** Representative immunoblotting and qPCR of NSUN2 and TRIM28 in TRIM28-knockdown and control 22Rv1 cells, with or without NSUN2 overexpression. **K** Representative images and quantification of the colony formation assay in TRIM28-knockdown and control 22Rv1 cells, with or without NSUN2 overexpression. **L** Quantification of CCK-8 proliferation assays in TRIM28-knockdown and control 22Rv1 cells, with or without NSUN2 overexpression.

Construction of stable knockdown and overexpressed cells

Lentiviruses were acquired from Genechem (China) to create stable cell models in C4-2 and 22Rv1. Cells suffered 3 μg/mL puromycin (MCE, USA) selection for 5 days following lentivirus transfection. Western blot and RT-qPCR were applied to measure transfection efficiency, with targeted sequences listed in the Additional file.

Luciferase reporter assay

cDNAs were inserted into pGL4.10 control vectors (Promega)[115]. The inserted sequences are outlined in the Additional file. 293T cells underwent transfection with FOXA1 plasmid, pRL-TK plasmids, and luciferase reporter plasmid. Cells were harvested after 48 h to assess luciferase activity.

Statistical analysis

GraphPad Prism 9.0 was utilized for data analysis. We used the Student's *t* test to assess how significant the differences were. Statistical significance is indicated by *P* values less than 0.05. ($^{*}p < 0.05$, $^{**}p < 0.01$, and $^{***}p < 0.001$).

Data availability

The following describes the transcriptome data and clinical data of 533 PRAD samples from 2 cohorts: 497 PRAD samples from TCGA (https://www.cancer.gov/about-nci/organization/ccg/research/structural-genomics/tcga), 36 PRAD samples from GSE46602 (https://www.ncbi.nlm.nih.gov/geo/query/acc.cgi). The other data supporting the findings of this study are available from the corresponding author upon reasonable request.

Code availability

The R code used for statistical analysis and figure generation in this study is available upon request. Interested researchers are encouraged to contact the corresponding author, and the necessary files will be provided promptly.

Received: 7 October 2024; Accepted: 6 April 2025;
Published online: 03 May 2025

References

1. Liu, Y. et al. Osteoblast-derived exosomal miR-140-3p targets ACER2 and increases the progression of prostate cancer via the AKT/mTOR pathway-mediated inhibition of autophagy. *FASEB j.* **38**, e70206 (2024).
2. Xuan, Z. et al. NDR1/FBXO11 promotes phosphorylation-mediated ubiquitination of β-catenin to suppress metastasis in prostate cancer. *Int. J. Biol. Sci.* **20**, 4957–4977 (2024).
3. Shen, M. M. & Abate-Shen, C. Molecular genetics of prostate cancer: new prospects for old challenges. *Genes Dev.* **24**, 1967–2000 (2010).
4. Logothetis, C. J. et al. Molecular classification of prostate cancer progression: foundation for marker-driven treatment of prostate cancer. *Cancer Discov.* **3**, 849–861 (2013).
5. Ge, R. et al. Epigenetic modulations and lineage plasticity in advanced prostate cancer. *Ann. Oncol.***31**, 470–479 (2020).
6. Rebello, R. J. et al. Prostate cancer. *Nat Rev. Dis Primers* **7**, 9 (2021).
7. Klotz, L. et al. Nadir testosterone within first year of androgen-deprivation therapy (ADT) predicts for time to castration-resistant progression: a secondary analysis of the PR-7 trial of intermittent versus continuous ADT. *J. Clin. Oncol.***33**, 1151–1156 (2015).
8. Ryan, C. J. et al. Abiraterone in metastatic prostate cancer without previous chemotherapy. *N. Engl. J. Med.* **368**, 138–148 (2013).
9. Scher, H. I. et al. Increased survival with enzalutamide in prostate cancer after chemotherapy. *N. Engl. J. Med.* **367**, 1187–1197 (2012).
10. Beer, T. M. et al. Enzalutamide in metastatic prostate cancer before chemotherapy. *N. Engl. J. Med.* **371**, 424–433 (2014).
11. Smith, M. R. et al. Apalutamide treatment and metastasis-free survival in prostate cancer. *N. Engl. J. Med.* **378**, 1408–1418 (2018).
12. Smith, M. R. et al. Darolutamide and survival in metastatic, hormone-sensitive prostate cancer. *N. Engl. J. Med.* **386**, 1132–1142 (2022).
13. Dai, B. et al. CACA guidelines for holistic integrative management of prostate cancer. *Holist. Integr. Oncol.* **3**, 47 (2024).
14. Watson, P. A., Arora, V. K. & Sawyers, C. L. Emerging mechanisms of resistance to androgen receptor inhibitors in prostate cancer. *Nat. Rev. Cancer* **15**, 701–711 (2015).
15. Deng, S. et al. Ectopic JAK-STAT activation enables the transition to a stem-like and multilineage state conferring AR-targeted therapy resistance. *Nat. Cancer* **3**, 1071–1087 (2022).
16. Mateo, J. et al. DNA-repair defects and olaparib in metastatic prostate cancer. *N. Engl. J. Med* **373**, 1697–1708 (2015).
17. Malumbres, M. & Barbacid, M. Cell cycle, CDKs and cancer: a changing paradigm. *Nat. Rev. Cancer* **9**, 153–166 (2009).
18. Sallman, D. A. et al. Eprenetapopt (APR-246) and azacitidine in TP53-mutant myelodysplastic syndromes. *J. Clin. Oncol.* **39**, 1584–1594 (2021).
19. Crabb, S. J. et al. ProCAID: a phase I clinical trial to combine the AKT inhibitor AZD5363 with docetaxel and prednisolone chemotherapy for metastatic castration-resistant prostate cancer. *Investig. N. Drugs* **35**, 599–607 (2017).
20. Lasko, L. M. et al. Discovery of a selective catalytic p300/CBP inhibitor that targets lineage-specific tumours. *Nature* **550**, 128–132 (2017).
21. Piha-Paul, S. A. et al. First-in-human study of mivebresib (ABBV-075), an oral pan-inhibitor of bromodomain and extra terminal proteins, in patients with relapsed/refractory solid tumors. *Clin. Cancer Res.***25**, 6309–6319 (2019).
22. Chen, X. et al. 5-methylcytosine promotes pathogenesis of bladder cancer through stabilizing mRNAs. *Nat. Cell Biol.* **21**, 978–990 (2019).
23. Li, P. et al. The m(5) C methyltransferase NSUN2 promotes codon-dependent oncogenic translation by stabilising tRNA in anaplastic thyroid cancer. *Clin. Transl. Med.* **13**, e1466 (2023).
24. Barbieri, I. & Kouzarides, T. Role of RNA modifications in cancer. *Nat. Rev. Cancer* **20**, 303–322 (2020).
25. Wang, Y. et al. Aberrant m5C hypermethylation mediates intrinsic resistance to gefitinib through NSUN2/YBX1/QSOX1 axis in EGFR-mutant non-small-cell lung cancer. *Mol. Cancer* **22**, 81 (2023).

26. Chen, T. et al. NSUN2 is a glucose sensor suppressing cGAS/STING to maintain tumorigenesis and immunotherapy resistance. *Cell Metab.* **35**, 1782–1798.e8 (2023).
27. Delaunay, S. et al. Mitochondrial RNA modifications shape metabolic plasticity in metastasis. *Nature* **607**, 593–603 (2022).
28. Li, Y. et al. TET2-mediated mRNA demethylation regulates leukemia stem cell homing and self-renewal. *Cell Stem Cell* **30**, 1072–1090.e10 (2023).
29. Yang, H. et al. FMRP promotes transcription-coupled homologous recombination via facilitating TET1-mediated m5C RNA modification demethylation. *Proc. Natl. Acad. Sci. USA* **119**, e2116251119 (2022).
30. Chen, M. et al. RNA N6-methyladenosine methyltransferase-like 3 promotes liver cancer progression through YTHDF2-dependent posttranscriptional silencing of SOCS2. *Hepatology***67**, 2254–2270 (2018).
31. Lin, X. et al. RNA m6A methylation regulates the epithelial mesenchymal transition of cancer cells and translation of Snail. *Nat. Commun.* **10**, 2065 (2019).
32. Nie, S. et al. ALKBH5-HOXA10 loop-mediated JAK2 m6A demethylation and cisplatin resistance in epithelial ovarian cancer. *J. Exp. Clin. Cancer Res.***40**, 284 (2021).
33. Lan, Q. et al. The emerging roles of RNA m6A methylation and demethylation as critical regulators of tumorigenesis, drug sensitivity, and resistance. *Cancer Res.* **81**, 3431–3440 (2021).
34. Sahu, B. et al. Dual role of FoxA1 in androgen receptor binding to chromatin, androgen signalling and prostate cancer. *EMBO J.* **30**, 3962–3976 (2011).
35. Gerhardt, J. et al. FOXA1 promotes tumor progression in prostate cancer and represents a novel hallmark of castration-resistant prostate cancer. *Am. J. Pathol.* **180**, 848–861 (2012).
36. Barbieri, C. E. et al. Exome sequencing identifies recurrent SPOP, FOXA1 and MED12 mutations in prostate cancer. *Nat. Genet.* **44**, 685–689 (2012).
37. Grasso, C. S. et al. The mutational landscape of lethal castration-resistant prostate cancer. *Nature* **487**, 239–243 (2012).
38. He, Y. et al. FOXA1 overexpression suppresses interferon signaling and immune response in cancer. *J. Clin. Investig.* **131**, e147025 (2021).
39. Jin, H.-J. et al. Androgen receptor-independent function of FoxA1 in prostate cancer metastasis. *Cancer Res.* **73**, 3725–3736 (2013).
40. Wang, X. et al. FOXA1 inhibits hypoxia programs through transcriptional repression of HIF1A. *Oncogene* **41**, 4259–4270 (2022).
41. Song, B. et al. Targeting FOXA1-mediated repression of TGF-β signaling suppresses castration-resistant prostate cancer progression. *J. Clin. Investig.* **129**, 569–582 (2019).
42. Lupien, M. et al. FoxA1 translates epigenetic signatures into enhancer-driven lineage-specific transcription. *Cell* **132**, 958–970 (2008).
43. Pomerantz, M. M. et al. The androgen receptor cistrome is extensively reprogrammed in human prostate tumorigenesis. *Nat. Genet.* **47**, 1346–1351 (2015).
44. Gao, S. et al. Forkhead domain mutations in FOXA1 drive prostate cancer progression. *Cell Res.* **29**, 770–772 (2019).
45. Del Giudice, M. et al. FOXA1 regulates alternative splicing in prostate cancer. *Cell Rep.* **40**, 111404 (2022).
46. Rebello, R. J. et al. Prostate cancer. *Nat. Rev. Dis. Prim.* **7**, 9 (2021).
47. Dang, C. V. et al. Drugging the 'undruggable' cancer targets. *Nat. Rev. Cancer* **17**, 502–508 (2017).
48. Wang, S. et al. High throughput chemical screening reveals multiple regulatory proteins on FOXA1 in breast cancer cell lines. *Int. J. Mol. Sci.* **19**, 4123 (2018).
49. Arrowsmith, C. H. et al. Epigenetic protein families: a new frontier for drug discovery. *Nat. Rev. Drug Discov.* **11**, 384–400 (2012).
50. Gao, S. et al. Chromatin binding of FOXA1 is promoted by LSD1-mediated demethylation in prostate cancer. *Nat. Genet.* **52**, 1011–1017 (2020).
51. Jin, J.-O. et al. Sequential ubiquitination of p53 by TRIM28, RLIM, and MDM2 in lung tumorigenesis. *Cell Death Differ.* **28**, 1790–1803 (2021).
52. Xu, W. et al. METTL3 regulates heterochromatin in mouse embryonic stem cells. *Nature* **591**, 317–321 (2021).
53. Agarwal, N. et al. TRIM28 is a transcriptional activator of the mutant TERT promoter in human bladder cancer. *Proc. Natl. Acad. Sci. USA*. **118**, (2021).
54. Lin, J. et al. The SETDB1-TRIM28 complex suppresses antitumor immunity. *Cancer Immunol. Res.* **9**, 1413–1424 (2021).
55. Park, H.-H. et al. RIPK3 activation induces TRIM28 derepression in cancer cells and enhances the anti-tumor microenvironment. *Mol. Cancer* **20**, 107 (2021).
56. The Cancer Genome Atlas Research Network. The molecular taxonomy of primary prostate cancer. *Cell***163**: 1011–1025 (2015).
57. Cui, J. et al. TRIM28 protects CARM1 from proteasome-mediated degradation to prevent colorectal cancer metastasis. *Sci. Bull.* **64**, 986–997 (2019).
58. Fong, K.-W. et al. TRIM28 protects TRIM24 from SPOP-mediated degradation and promotes prostate cancer progression. *Nat. Commun.* **9**, 5007 (2018).
59. Yende, A. S. et al. TRIM28 promotes luminal cell plasticity in a mouse model of prostate cancer. *Oncogene* **42**, 1347–1359 (2023).
60. Huang, Z. et al. SETDB1 modulates degradation of phosphorylated Rb and anticancer efficacy of CDK4/6 inhibitors. *Cancer Res.* **83**, 875–889 (2023).
61. Xu, Y. et al. ZNF397 deficiency triggers TET2-driven lineage plasticity and AR-targeted therapy resistance in prostate cancer. *Cancer Discov.* **14**, 1496–1521 (2024).
62. Yu, S. et al. MAGOH promotes gastric cancer progression via hnRNPA1 expression inhibition-mediated RONΔ160/PI3K/AKT signaling pathway activation. *J. Exp. Clin. Cancer Res.* **43**, 32 (2024).
63. Wang, L. et al. YTHDF2 inhibition potentiates radiotherapy antitumor efficacy. *Cancer Cell* **41**, 1294–1308.e8 (2023).
64. Yang, F. et al. Ferroptosis heterogeneity in triple-negative breast cancer reveals an innovative immunotherapy combination strategy. *Cell Metab.* **35**, 84–100.e8 (2023).
65. Wasserman, W. W. & Sandelin, A. Applied bioinformatics for the identification of regulatory elements. *Nat. Rev. Genet.* **5**, 276–287 (2004).
66. Wang, J. et al. GLUT1 is an AR target contributing to tumor growth and glycolysis in castration-resistant and enzalutamide-resistant prostate cancers. *Cancer Lett.* **485**, 45–55 (2020).
67. Lippman, S. M. & Hawk, E. T. Cancer prevention: from 1727 to milestones of the past 100 years. *Cancer Res.* **69**, 5269–5284 (2009).
68. Løvf, M. et al. Multifocal primary prostate cancer exhibits high degree of genomic heterogeneity. *Eur. Urol.* **75**, 498–505 (2019).
69. Wahida, A. et al. The coming decade in precision oncology: six riddles. *Nat. Rev. Cancer* **23**, 43–54 (2023).
70. Siegel, R. L. et al. Cancer statistics, 2023. *CA: Cancer J. Clin.***73**, 17–48 (2023).
71. Harris, W. P. et al. Androgen deprivation therapy: progress in understanding mechanisms of resistance and optimizing androgen depletion. *Nat. Clin. Pract. Urol.* **6**, 76–85 (2009).
72. Linder, S. et al. Drug-induced epigenomic plasticity reprograms circadian rhythm regulation to drive prostate cancer toward androgen independence. *Cancer Discov.* **12**, 2074–2097 (2022).
73. Fraser, M. et al. Genomic hallmarks of localized, non-indolent prostate cancer. *Nature* **541**, 359–364 (2017).
74. Blee, A. M. et al. TMPRSS2-ERG controls luminal epithelial lineage and antiandrogen sensitivity in PTEN and TP53-mutated prostate cancer. *Clin. Cancer Res.***24**, 4551–4565 (2018).

75. Stopsack, K. H. et al. Oncogenic genomic alterations, clinical phenotypes, and outcomes in metastatic castration-sensitive prostate cancer. *Clin. Cancer Res.***26**, 3230–3238 (2020).
76. Abida, W. et al. Genomic correlates of clinical outcome in advanced prostate cancer. *Proc. Natl Acad. Sci. USA* **116**, 11428–11436 (2019).
77. Gao, J. et al. Integrative analysis of complex cancer genomics and clinical profiles using the cBioPortal. *Sci. Signal.* **6**, pl1 (2013).
78. Cerami, E. et al. The cBio cancer genomics portal: an open platform for exploring multidimensional cancer genomics data. *Cancer Discov.* **2**, 401–404 (2012).
79. Hou, G. et al. SUMOylation of YTHDF2 promotes mRNA degradation and cancer progression by increasing its binding affinity with m6A-modified mRNAs. *Nucleic Acids Res.* **49**, 2859–2877 (2021).
80. Liu, T. et al. The m6A reader YTHDF1 promotes ovarian cancer progression via augmenting EIF3C translation. *Nucleic Acids Res.* **48**, 3816–3831 (2020).
81. Wang, Q. et al. METTL3-mediated m6A modification of HDGF mRNA promotes gastric cancer progression and has prognostic significance. *Gut* **69**, 1193–1205 (2020).
82. Guan, Q. et al. Functions, mechanisms, and therapeutic implications of METTL14 in human cancer. *J. Hematol. Oncol.* **15**, 13 (2022).
83. Chang, G. et al. YTHDF3 induces the translation of m6A-enriched gene transcripts to promote breast cancer brain metastasis. *Cancer Cell*. **38**, 857-871.e7 (2020).
84. Chen, H. et al. RNA N6-methyladenosine methyltransferase METTL3 facilitates colorectal cancer by activating the m6A-GLUT1-mTORC1 Axis and is a therapeutic target. *Gastroenterology*. **160**, 1284-1300.e16 (2021).
85. Hu, Y. et al. NSUN2 modified by SUMO-2/3 promotes gastric cancer progression and regulates mRNA m5C methylation. *Cell Death Dis.* **12**, 842 (2021).
86. Su, J. et al. NSUN2-mediated RNA 5-methylcytosine promotes esophageal squamous cell carcinoma progression via LIN28B-dependent GRB2 mRNA stabilization. *Oncogene* **40**, 5814–5828 (2021).
87. Niu, X. et al. A cis-eQTL in NSUN2 promotes esophageal squamous-cell carcinoma progression and radiochemotherapy resistance by mRNA-m5C methylation. *Signal Transduct. Target. Ther.* **7**, 267 (2022).
88. Chen, S.-Y. et al. RNA bisulfite sequencing reveals NSUN2-mediated suppression of epithelial differentiation in pancreatic cancer. *Oncogene* **41**, 3162–3176 (2022).
89. Sun, Z. et al. Aberrant NSUN2-mediated m5C modification of H19 lncRNA is associated with poor differentiation of hepatocellular carcinoma. *Oncogene* **39**, 6906–6919 (2020).
90. Sun, G. et al. Multi-omics analysis of expression and prognostic value of NSUN members in prostate cancer. *Front. Oncol.* **12**, 965571 (2022).
91. Luo, G. et al. NSUN2-mediated RNA m5C modification modulates uveal melanoma cell proliferation and migration. *Epigenetics* **17**, 922–933 (2022).
92. Wang, N. et al. m5C-dependent cross-regulation between nuclear reader ALYREF and writer NSUN2 promotes urothelial bladder cancer malignancy through facilitating RABL6/TK1 mRNAs splicing and stabilization. *Cell Death Dis.* **14**, 139 (2023).
93. Frye, M. & Watt, F. M. The RNA methyltransferase Misu (NSun2) mediates Myc-induced proliferation and is upregulated in tumors. *Curr. Biol.***16**, 971–981 (2006).
94. Yang, M. et al. NSUN2 promotes osteosarcoma progression by enhancing the stability of FABP5 mRNA via m5C methylation. *Cell Death Dis.* **14**, 125 (2023).
95. Adams, E. J. et al. FOXA1 mutations alter pioneering activity, differentiation and prostate cancer phenotypes. *Nature* **571**, 408–412 (2019).
96. Helminen, L. et al. Chromatin accessibility and pioneer factor FOXA1 restrict glucocorticoid receptor action in prostate cancer. *Nucleic Acids Res.* **52**, 625–642 (2024).
97. Addison, J. B. et al. KAP1 promotes proliferation and metastatic progression of breast cancer cells. *Cancer Res.* **75**, 344–355 (2015).
98. Chen, L. et al. Tripartite motif containing 28 (Trim28) can regulate cell proliferation by bridging HDAC1/E2F interactions. *J. Biol. Chem.* **287**, 40106–40118 (2012).
99. Liang, J. et al. Verteporfin inhibits PD-L1 through autophagy and the STAT1-IRF1-TRIM28 signaling axis, exerting antitumor efficacy. *Cancer Immunol. Res.* **8**, 952–965 (2020).
100. Ma, X. et al. TRIM28 promotes the escape of gastric cancer cells from immune surveillance by increasing PD-L1 abundance. *Signal Transduct. Target. Ther.* **8**, 246 (2023).
101. Zhang, F.-L. et al. Dynamic SUMOylation of MORC2 orchestrates chromatin remodelling and DNA repair in response to DNA damage and drives chemoresistance in breast cancer. *Theranostics* **13**, 973–990 (2023).
102. Yang, Y. et al. HIF-1 Interacts with TRIM28 and DNA-PK to release paused RNA polymerase II and activate target gene transcription in response to hypoxia. *Nat. Commun.* **13**, 316 (2022).
103. Pineda, C. T. & Potts, P. R. Oncogenic MAGEA-TRIM28 ubiquitin ligase downregulates autophagy by ubiquitinating and degrading AMPK in cancer. *Autophagy* **11**, 844–846 (2015).
104. Sun, Y. et al. A dissection of oligomerization by the TRIM28 tripartite motif and the interaction with members of the Krab-ZFP family. *J. Mol. Biol.* **431**, 2511–2527 (2019).
105. Tan, Q. et al. miR-125b-5p upregulation by TRIM28 induces cisplatin resistance in non-small cell lung cancer through CREB1 inhibition. *BMC Pulm. Med.* **22**, 469 (2022).
106. Van Tilborgh, N. et al. The transcription intermediary factor 1β coactivates the androgen receptor. *J. Endocrinol. Investig.* **36**, 699–706 (2013).
107. Golding, S. E. et al. Dynamic inhibition of ATM kinase provides a strategy for glioblastoma multiforme radiosensitization and growth control. *Cell Cycle* **11**, 1167–1173 (2012).
108. Damineni, S. et al. Expression of tripartite motif-containing protein 28 in primary breast carcinoma predicts metastasis and is involved in the stemness, chemoresistance, and tumor growth. *Tumour Biol.* **39**, 1010428317695919 (2017).
109. Liang, M. et al. E3 ligase TRIM28 promotes anti-PD-1 resistance in non-small cell lung cancer by enhancing the recruitment of myeloid-derived suppressor cells. *J. Exp. Clin. Cancer Res.* **42**, 275 (2023).
110. Ratnadiwakara, M. & Änkö, M.-L. mRNA stability assay using transcription inhibition by actinomycin D in mouse pluripotent stem cells. *Bio-Protoc.* **8**, e3072 (2018).
111. Ma, H. L. et al. SRSF2 plays an unexpected role as reader of m(5)C on mRNA, linking epitranscriptomics to cancer. *Mol. Cell* **83**, 4239–4254.e10 (2023).
112. Xiuzhi Wang, M. W. et al. RNA 5-methylcytosine regulates YBX2-dependent liquid-liquid phase separation. *Fundam. Res.* **2**, 48–55 (2022).
113. Dai, X. et al. YTHDF2 Binds to 5-methylcytosine in RNA and modulates the maturation of ribosomal RNA. *Anal. Chem.* **92**, 1346–1354 (2020).
114. Chen, H. et al. m(5)C modification of mRNA serves a DNA damage code to promote homologous recombination. *Nat. Commun.* **11**, 2834 (2020).
115. Yang, X. et al. 5-methylcytosine promotes mRNA export - NSUN2 as the methyltransferase and ALYREF as an mC reader. *Cell Res.* **27**, 606–625 (2017).

Acknowledgements

We appreciate Dr. Wenhao Xu's insightful suggestions on the presentation and design of the research in the article. We thank Bullet Edits for language

editing service. We thanked Dr. Zhesheng Chen for the critical comments on the results of figures. This work is supported by Grants from the National Natural Science Foundation of China (Nos. 82473505 and 81902568), Shanghai Science and Technology Committee (Nos. 20ZR1413100, 18511108000).

Author contributions

Zhen-da Wang: Writing – original draft, Validation, Methodology, Investigation, Funding acquisition. Abudurexiti Mierxiati: Writing – original draft, Methodology, Investigation. Tian Li and Wen-kai Zhu: Methodology. Hua Xu: Writing—review & editing, Methodology, Supervision Fangning Wan: Writing—review & editing, Methodology, Supervision, Funding acquisition. Ding-wei Ye: Review & editing, Supervision, Funding acquisition.

Competing interests

The authors declare no competing interests.

Ethics approval

The procedures for tumor xenografts were carried out according to the approved protocol by The Institutional Animal Care and Use Committee at Fudan University. Each patient provided written informed consent prior to the obtaining of tumor tissue, and the procedure was executed in compliance with institutional and state laws governing the use of human tissues for experimental purposes.

Consent for publication

The study was carried out in strict accordance with the principles enshrined in the Declaration of Helsinki, and was approved by the Medical Ethics Committee of Cancer Hospital, Fudan University (SCCIRB). Written informed consent was acquired from all participants.

Additional information

Supplementary information The online version contains supplementary material available at https://doi.org/10.1038/s41698-025-00904-x.

Correspondence and requests for materials should be addressed to Tian Li, Hua Xu, Fangning Wan or Dingwei Ye.